Supplemental Document

OPTICA

Terahertz-wave decoding of femtosecond extreme-ultraviolet light pulses: supplement

I. Ilyakov,[1,†] N. Agarwal,[2,3,4,5,†] J.-C. Deinert,[1] J. Liu,[2] A. Yaroslavtsev,[2,6] L. Foglia,[7] G. Kurdi,[7] R. Mincigrucci,[7] E. Principi,[7] G. Jakob,[8] M. Kläui,[8] T. S. Seifert,[9,10] T. Kampfrath,[9,10] S. Kovalev,[1,13] R. E. Carley,[2,14] A. O. Scherz,[2] and M. Gensch[11,12,15]

[1] *Institute of Radiation Physics, Helmholtz-Zentrum Dresden-Rossendorf, Bautzner Landstr. 400, 01328 Dresden, Germany*
[2] *European XFEL, Holzkoppel 4, 22869 Schenefeld, Germany*
[3] *Max Planck Institute for the Structure and Dynamics of Matter, Luruper Chaussee 149, 22761 Hamburg, Germany*
[4] *Department of Physics, Universität Hamburg, Jungiusstraße 9, 20355 Hamburg, Germany*
[5] *Institute of Physics and Astronomy (IFA), Aarhus University, Ny Munkegade 120, 8000 Aarhus C, Denmark*
[6] *Department of Physics and Astronomy, Uppsala University, PO Box 516, 75120 Uppsala, Sweden*
[7] *Elettra-Sincrotrone Trieste S.C.p.A., 34149 Basovizza, Trieste, Italy*
[8] *Johannes Gutenberg University Mainz, Institute of Physics, Staudinger Weg 7, 55128 Mainz, Germany*
[9] *Department of Physics, Freie Universität Berlin, Arnimallee 14, 14195 Berlin, Germany*
[10] *Fritz Haber Institute of the Max Planck Society, Faradayweg 4-6, 14195 Berlin, Germany*
[11] *Institute of Optical Sensor Systems, DLR (German Aerospace Center), Rutherfordstr. 2, 12489 Berlin, Germany*
[12] *Institute of Optics and Atomic Physics, Technische Universität Berlin, Strasse des 17. Juni 135, 10623 Berlin, Germany*
[13] *e-mail: s.kovalev@hzdr.de*
[14] *e-mail: robert.carley@xfel.eu*
[15] *e-mail: michael.gensch@dlr.de*
[†] *These authors contributed equally to this work.*

Supplement DOI: https://doi.org/10.6084/m9.figshare.19596802

Parent Article DOI: https://doi.org/10.1364/OPTICA.453130

Supplementary Information

Terahertz-wave decoding of femtosecond extreme-ultraviolet light pulses

I. Ilyakov[+1], N. Agarwal[+2,3,4,5], J.-C. Deinert[1], J. Liu[2], A. Yaroslavtsev[2,6], L. Foglia[7], G. Kurdi[7], R. Mincigrucci[7], E. Principi[7], G. Jakob[8], M. Kläui[8], T. S. Seifert[9,10], T. Kampfrath[9,10], S. Kovalev[*1], R. E. Carley[*2], A. O. Scherz[2], M. Gensch[*11,12]

1. Institute of Radiation Physics, Helmholtz-Zentrum Dresden-Rossendorf, Bautzner Landstr. 400, 01328 Dresden, Germany

2. European X-Ray Free Electron Laser Facility, Holzkoppel 4, 22869 Schenefeld, Germany

3. Max Planck Institute for the Structure and Dynamics of Matter, Luruper Chaussee 149, 22761 Hamburg, Germany

4. Universität Hamburg, Department of Physics, Jungiusstraße 9, 20355 Hamburg, Germany

5. Institute of Physics and Astronomy (IFA), Aarhus University, Ny Munkegade 120, 8000 Aarhus C, Denmark

6. Uppsala University, Department of Physics and Astronomy, PO Box 516, 75120 Uppsala, Sweden

7. Elettra-Sincrotrone Trieste S.C.p.A., 34149 Basovizza, Trieste, Italy

8. Johannes Gutenberg University Mainz, Institute of Physics, Staudinger Weg 7, 55128 Mainz, Germany

9. Freie Universität Berlin, Fachbereich Physik, Arnimallee 14, 14195 Berlin, Germany

10. Fritz Haber Institute of the Max Planck Society, Faradayweg 4-6, 14195 Berlin, Germany

11. Institute of Optical Sensor Systems, DLR (German Aerospace Center), Rutherfordstr. 2 12489 Berlin, Germany

12. TU Berlin, Institute of Optics and Atomic Physics, Strasse des 17. Juni 135, 10623 Berlin, Germany

1. Calibration of the arrival-time monitor

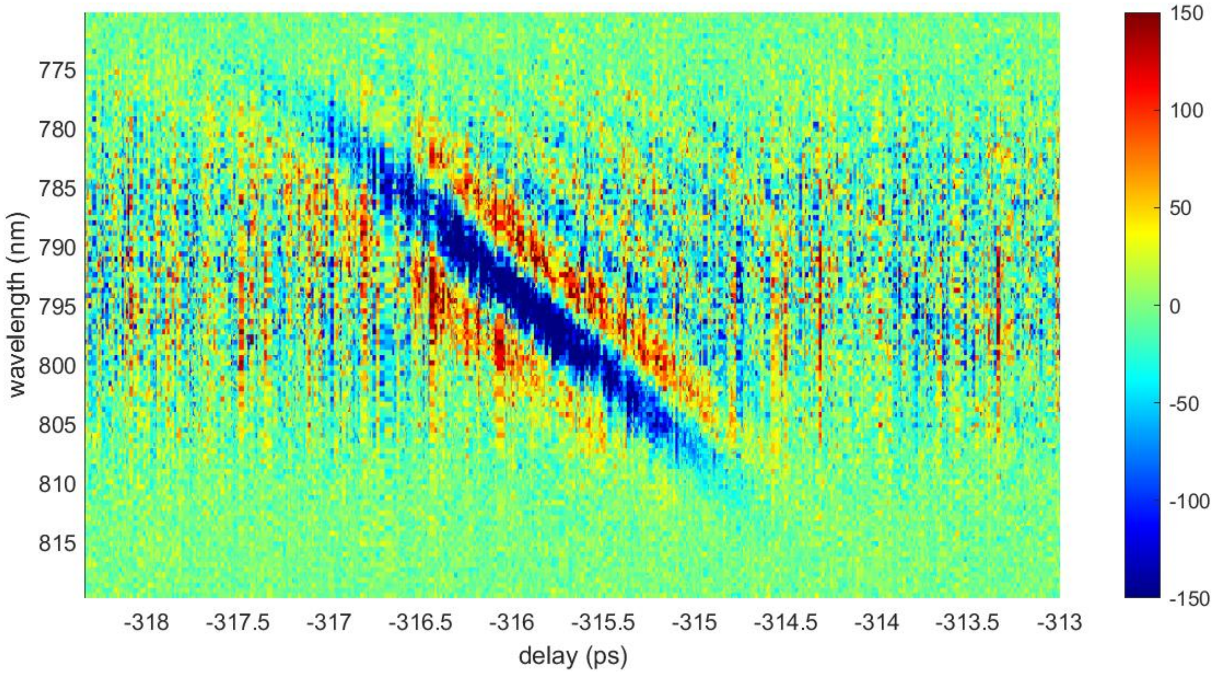

Supplementary Figure S1a. Single-shot spectra with different delays adjusted via the optical delay line.

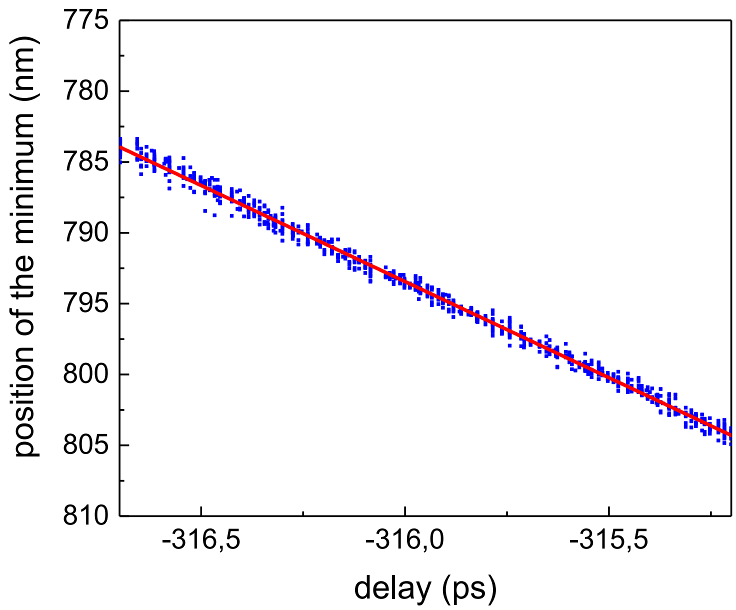

Supplementary Figure S1b. Position of the main minimum in nm vs delay in ps.

Our experimental setup is shown in the main text **figure 1a**. In the experiments the arrival time of the probe laser pulses with respect to the XUV pulses could be varied via a mechanical delay line. The XUV pulses, generated by a high-gain harmonic-generation (HGHG) seeding scheme (at 25 Hz repetition rate), were impacting at normal incidence onto a purpose-built spintronic terahertz-emitter consisting of a tri-layer of Pt/CoFeB/W nanolayers (2 nm/1.8 nm/2 nm, respectively) deposited on a 500 µm thick z-cut (001) sapphire substrate. The sample is magnetized in plane by a constant magnetic field of 100 mT. The generated THz pulse is detected in forward direction through the substrate. At 1THz (which is on the lower side of the emitted spectrum) and with a pump beam radius in the experiment of 4 mm we obtain an estimate of the divergence of the THz beam of $\theta \sim 0.24$ rad. After 50 cm of free space propagation, this moderately diverging THz beam was focused by a parabolic mirror with an approximate diameter of 3.8 cm and an effective focal length of 2 cm. At this position the beam size at a frequency of 1THz, obtained under the Gaussian beam approximation, is estimated to be 2.6 cm. We hence expect that most of the emitted THz radiation is actually collected.

The single-shot measurement of the generated THz pulses was performed via the spectral decoding technique. The horizontally polarized 1.6 ps-"chirped" 800 nm laser pulse (the originally 40 fs long laser pulse is chirped using SF7 glass to 1.6 ps) is overlapped in time and propagates collinearly through a [110]-cut 2mm ZnTe crystal with the vertically polarized THz pulse. The repetition rate of the laser pulses is 50 Hz where every second pulse is not superposed with the THz pulse (25Hz) and used for background subtraction. The THz pulse induces a transient birefringence in the ZnTe crystal via the linear electro-optic effect (Pockels effect) proportional to the strength of its electric field. The induced ellipticity of the spectral components of the transmitted probe pulse is thereafter analyzed with a polarizer, quarter wave-plate and spectrometer. A more precise description of this single-shot THz detection method can be found elsewhere **[S1]**.

A set of THz single-shot measurements at various time delays between laser and XUV pulses is made in order to calibrate the change of the main extremum position encoded in optical wavelength versus time delay (supplementary **figure S1**). Based on these data a conversion coefficient of 13.5 nm/ps is determined.

2. Precision of the arrival time measurement

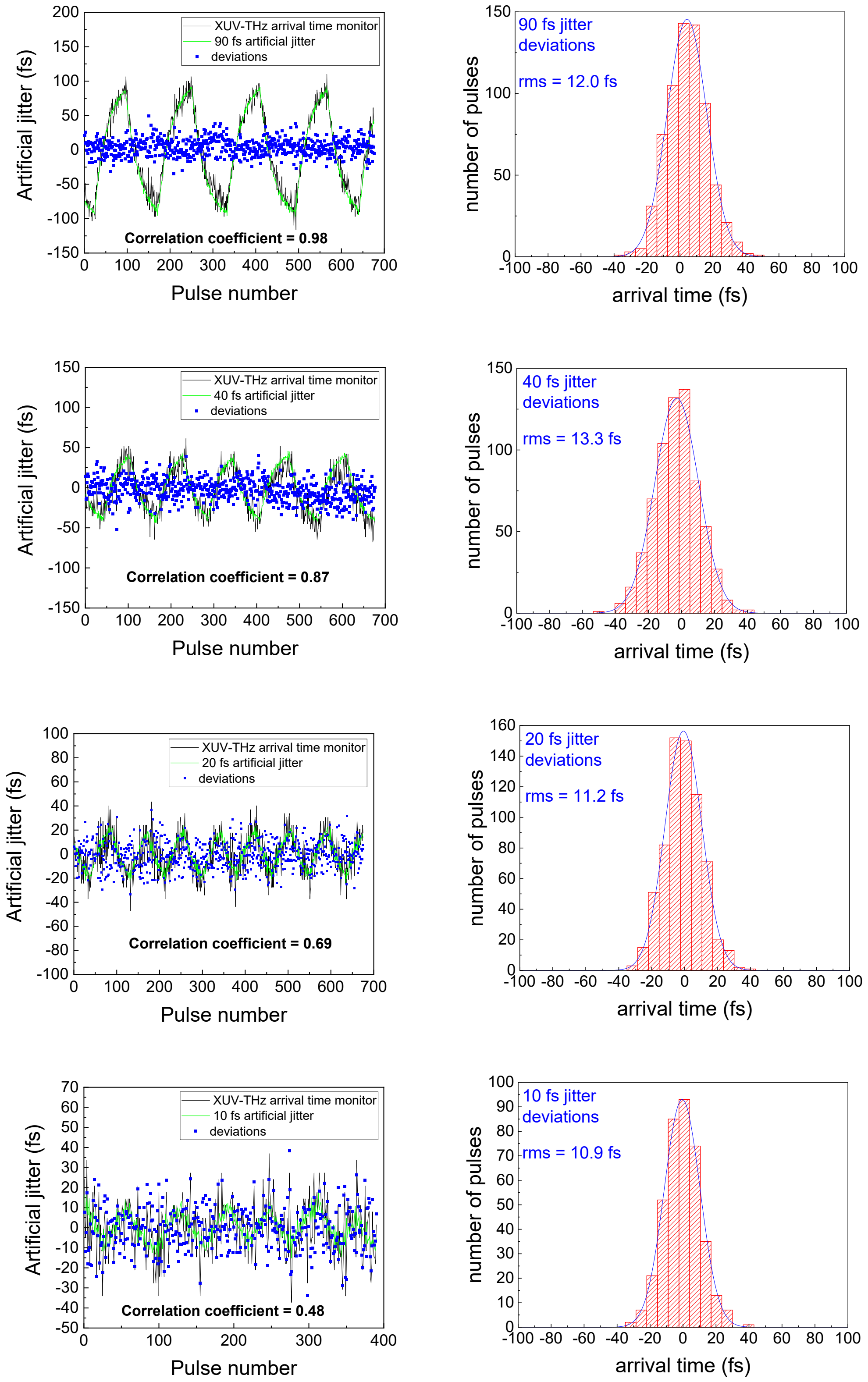

Supplementary Figure S2. (left column) Arrival time measurements (black line) with various artificially implemented approximate jitter values (green line) and their deviations (blue dots). **(right column)** Histogram plots of the deviations.

3. Dependence of the arrival-time monitor precision on the XUV pulse energy

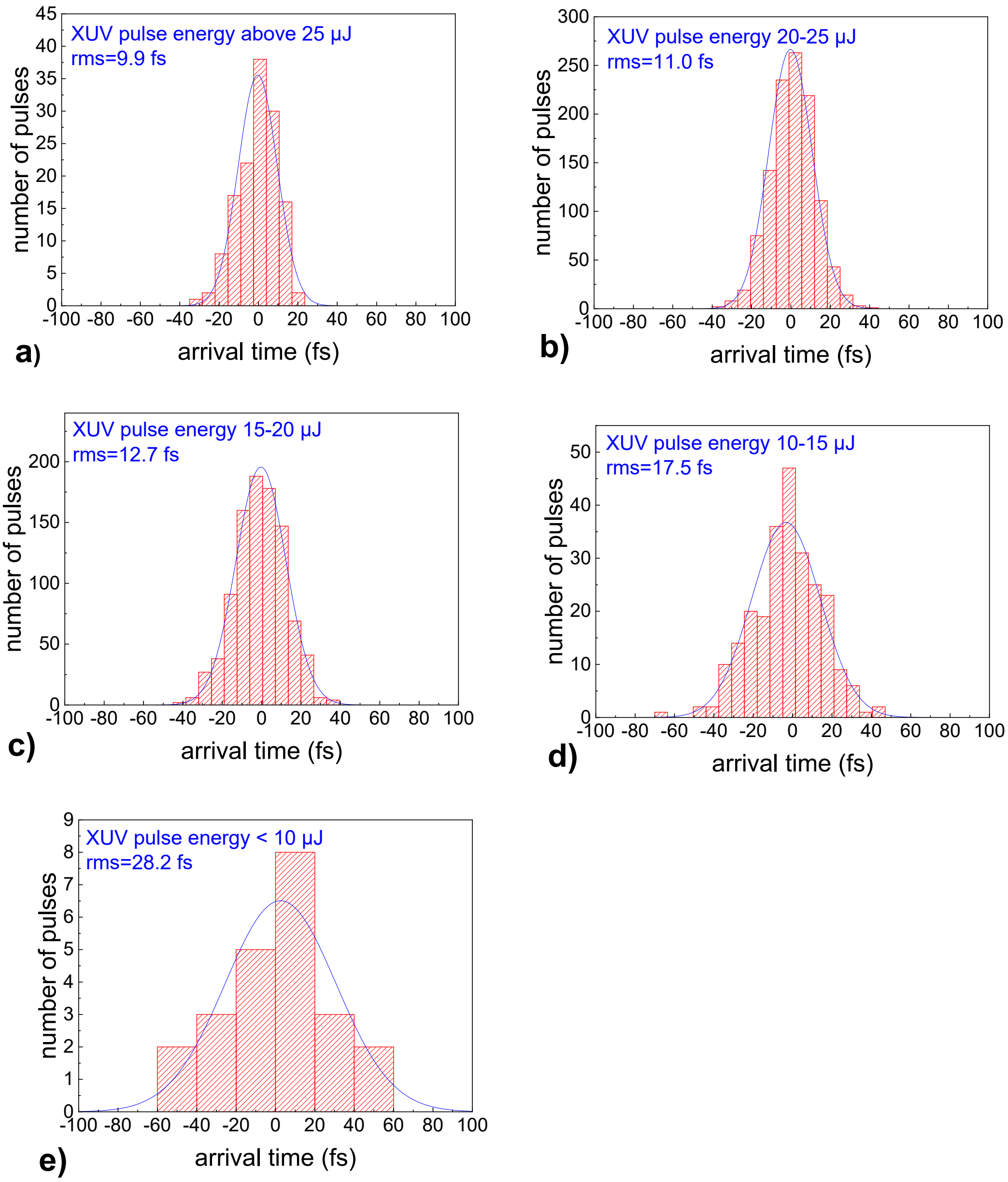

Supplementary Figure S3. Histograms of arrival times for XUV pulses with various energies (without artificial jitter): a) higher than 25 µJ, b) 20-25 µJ, c) 15-20 µJ, d) 10-15 µJ, e) lower than 10 µJ.

The arrival time monitor measurements have been analyzed to elucidate whether a dependence on the XUV pulse energy is observed. As can be seen in figure S3 the determined arrival time fluctuations increase with decreasing XUV pulse energy. This finding confirms that our monitor concept is applicable for low energy XUV pulses but that the precision of the measurement is also decreased at low XUV pulse energies.

4. Precision of the XUV pulse energy determination

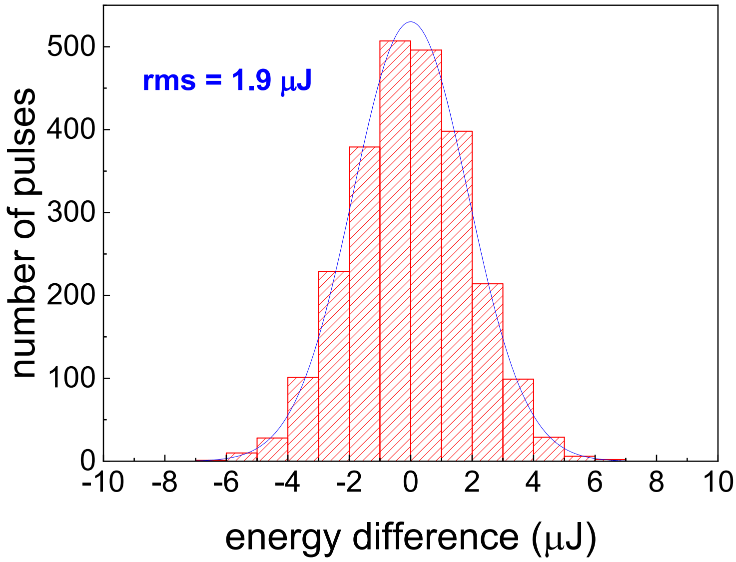

Supplementary Figure S4. Histogram of relative XUV pulse energies derived from the measurements shown in figure 3 of the main text. Plotted is the deviation of the THz amplitudes normalized to the XUV integral pulse energy.

The amplitudes of THz pulses generated during optical rectification are proportional to the energies of the excitation pulses. Therefore, this effect can be potentially used for the single-shot monitoring of the XUV pulse energies. In this experiment, we compare the XUV single-shot energies monitored by the FERMI XUV pulse energy monitor based on the photoionization of a rare gas with the amplitudes of the THz pulses generated in the STE. The single-shot amplitude of each THz pulse was normalized on the ratio of the mean value of FERMI XUV pulse energy monitor and of the mean value of THz amplitude averaged by 2499 pulses: $(E_{THz})_i \times \frac{(W_{FERMI})_{av}}{(E_{THz})_{av}}$. Here, *i* – is the pulse number, $(E_{THz})_i$ is the amplitude of each THz pulse, $(W_{FERMI})_{av}$ and $(E_{THz})_{av}$ are the average XUV pulse energy and the average amplitude of THz pulses. The results are presented in the main text in the figures 3a and 3b. Additionally, in the supplementary figure S4 a histogram of the deviations between two single-shot monitors is presented. It is seen that the rms is less than 2 μJ.

5. Simulations of THz waveforms and spectra

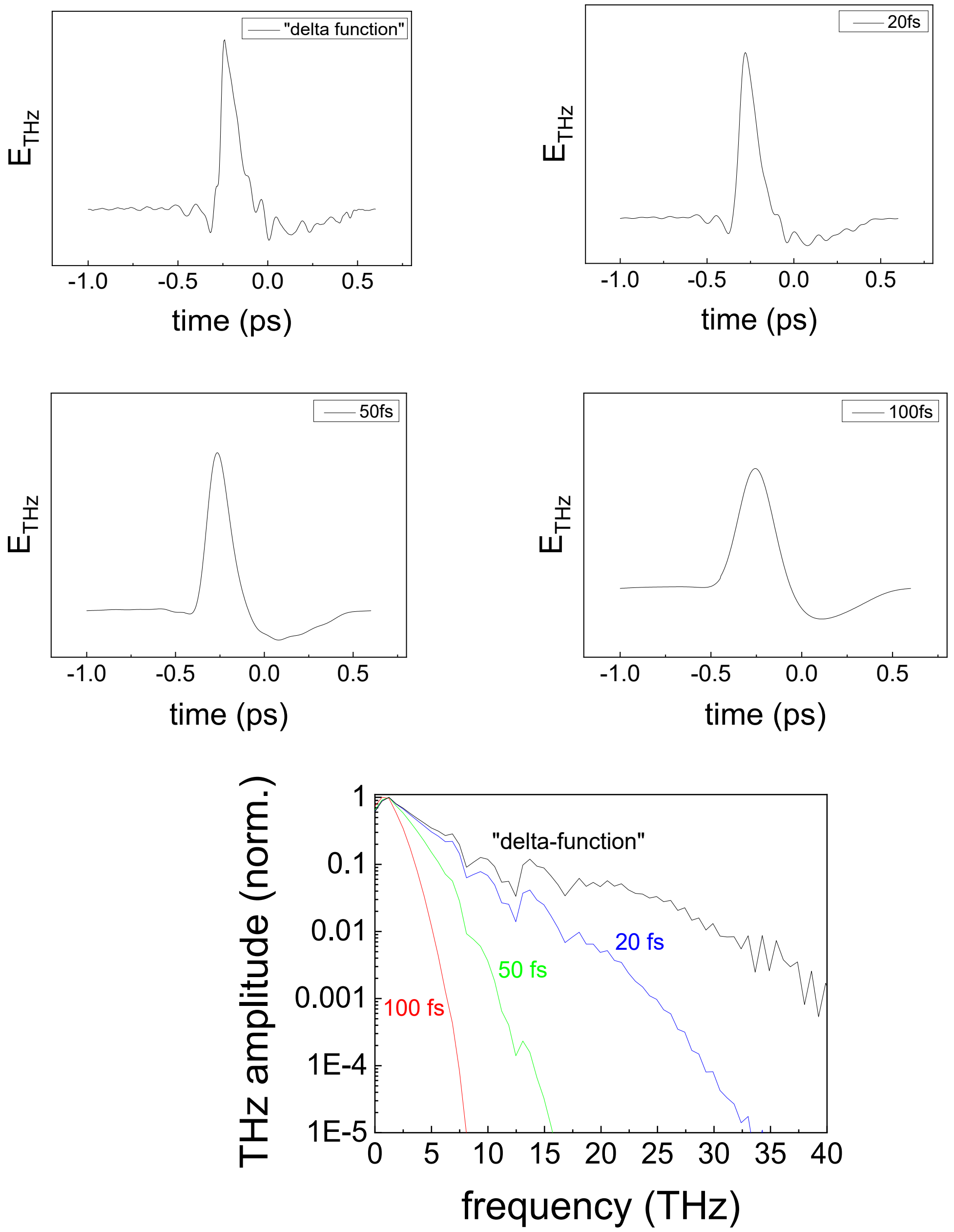

Supplementary Figure S5. An example of calculated THz time traces at the exit of the STE and their Fourier amplitude spectra are shown for excitation laser pulses with different pulse durations ("delta-function", 20 fs, 50 fs, 100 fs).

We performed calculations of THz time traces for laser pump-pulses with different pulse durations right behind the spintronic THz emitter. During the optical rectification process, the envelope of the excitation pulse is encoded into the emitted waveform, which allows the excitation pulse shape to be detected. In particular, the duration of the excitation pulse is included as a factor of $\exp(-\Omega^2\tau^2/4)$ into the expression for the spectrum of the emitted THz radiation, where Ω is the THz frequency and τ is the laser pulse duration. For the following, we assume that the electric field vs time as measured directly after the STE under excitation with

10 fs near-IR laser pulses represents the STE response to a “delta function”-like pulse. Convolving this delta-pulse response with the envelope of the laser pulses gives the time-domain response of the emitter for various pulse durations. In **Supplementary figure S5**, THz waveforms and their spectra for excitation pulses with various durations are presented. It is evident that the pump pulse duration strongly affects the waveform and spectrum of the emitted THz pulse. More complicated shapes like double-pulsed generation can also be determined from the measured waveform and the spectrum of the emitted pulses.

To calculate THz electric field at the position of the ZnTe detection crystal we took into account the focusing by the parabolic mirror (in the frequency domain the THz Fourier spectrum was multiplied by $i\Omega$, where i is the imaginary number, Ω is the THz frequency). To simulate the measured time trace we followed the results of **[S3, S4]**. The complex response function of the 2mm ZnTe crystal is influenced by the mismatch between the terahertz phase and the laser pulse group velocities, by the reflection of the terahertz pulse at the detection crystal surfaces, and by the absorption of the detected terahertz waves inside the crystal. Accounting for the parameters of the 2 mm ZnTe crystal **[S3-S5]**, the complex response function of the detector was derived. By taking a product of this function in the frequency domain with the complex-valued amplitude spectrum of the calculated THz electric field at the position of the ZnTe crystal, a good agreement with the experimental waveform was found (**figure 4** in the main text).

References

[S1] Z. Jiang, X.-C. Zhang, Electro-optic measurement of THz field pulses with a chirped optical beam, *Appl. Phys. Lett.* ***72***, 1945 (1998)

[S2] M.B. Danailov et al, Towards jitter-free pump-probe measurements at seeded free electron laser facilities, Opt. Express **22,** 12869 (2014)

[S3] H.J. Bakker et al., Distortion of terahertz pulses in electro-optic sampling, *J. Opt. Soc. Am. B* ***15***, 1795 (1998)

[S4] A. Leitenstorfer et al., Detectors and sources for ultrabroadband electro-optic sampling: Experiment and theory, *Appl. Phys. Lett.* ***74***, 1516 (1999)

[S5] M. M. Nazarov et al., The use of combination of nonlinear optical materials to control terahertz pulse generation and detection, *Appl. Phys. Lett.* ***92***, 021114 (2008)